PAPER

Check for updates

Room-temperature synthesis of bimetallic ZnCu-MOF-74 as an adsorbent for tetracycline removal from an aqueous solution†

Catalina V. Flores, ‡[a,b] Andy Machín-Garriga,‡[a] Juan L. Obeso, ‡[a,b]
J. Gabriel Flores,[d,e] Ilich A. Ibarra, [b,f] Nora S. Portillo-Vélez, *[c]
Carolina Leyva *[a] and Ricardo A. Peralta *[c]

The novel bimetallic MOF, ZnCu-MOF-74, has been evaluated for the remediation of tetracycline-contaminated water. ZnCu-MOF-74 was obtained at room temperature, avoiding high pressure and temperature. ZnCu-MOF-74 exhibited chemical stability in the 4–8 pH range. The adsorption result analysis was described using the Elovich kinetic model and the Langmuir adsorption isotherm, suggesting a physicochemical process. The maximum adsorption capacity was estimated at 775.66 mg g^{-1}. The pH of the solution and the presence of ions such as NO_3^-, SO_4^{2-}, Na^+, Mg^{2+}, Cl^-, and Ca^{2+} had no influence on the removal of tetracycline. In addition, π-interactions and metal complexation were proposed as possible adsorption mechanisms through FT-IR and XPS. ZnCu-MOF-74 showed outstanding cyclability performance, preserving its adsorption capacity after 4 adsorption–desorption cycles, besides exhibiting chemical stability, proving the benefits of applying ZnCu-MOF-74 in the water treatment process.

Introduction

Water quality has deteriorated worldwide due to the increase in pollution. This has displayed a negative impact on the environment and human life. The indiscriminate discharge of pollutants into aquatic ecosystems has escalated the risk of ecological and human health problems.[1] Water pollutants are generally classified as organic dyes, heavy metals, pesticides, disinfectants, and volatile organic compounds.[2] However, different water pollutants, such as pharmaceutical and personal care products, pesticides, and hormones, have emerged as relatively new contaminants.[3] An increase in their concentrations in a wide range of water bodies (rivers, lakes, and drinking water in urban areas) has been noted as a potential risk. The primary limitation in tackling this problem is the lack of monitoring and a long-term strategy.[4] Notably, one of the biggest concerns of our modern society is drug resistance, which is directly related to antimicrobial resistance caused by the presence of these pollutants in water, which could generate a global healthcare issue.[5]

Specifically, tetracycline (TC) is an antibiotic used for animal husbandry and human treatment. Nowadays, TC has been found in surface water.[6] Furthermore, the effective and efficient removal of TC from water systems is necessary. The adsorption process is one of the most practical and low-cost methods for removing water pollutants. Different materials, such as activated carbons,[7] metal oxides and zeolites have been applied for TC removal.[8] Porous materials called metal–organic frameworks (MOFs) have also been used for adsorption. MOFs are crystalline porous materials composed of organic units (linkers) and ion nodes (metals), displaying high surface area, well-defined metal distribution, and, in some cases, stability under water conditions.[9] Based on their improved properties, MOF materials have been employed for catalysis,[10] gas adsorption/separation,[11] and water harvesting.[12]

*a*Instituto Politécnico Nacional, CICATA U. Legaria, Laboratorio Nacional de Ciencia, Tecnología y Gestión Integrada del Agua (LNAgua), Legaria 694, Irrigación, 11500 Miguel Hidalgo, CDMX, Mexico. E-mail: zleyva@ipn.mx

*b*Laboratorio de Fisicoquímica y Reactividad de Superficies (LaFReS), Instituto de Investigaciones en Materiales, Universidad Nacional Autónoma de México, Circuito Exterior s/n, CU, Coyoacán, 04510 Ciudad de México, Mexico

*c*Departamento de Química, División de Ciencias Básicas e Ingeniería. Universidad Autónoma Metropolitana (UAM-I), 09340, Mexico. E-mail: rperalta@izt.uam.mx, noraportillo@xanum.uam.mx

*d*Departamento de Ingeniería de Procesos e Hidráulica, División de Ciencias Básicas e Ingeniería, Universidad Autónoma Metropolitana-Iztapalapa, 09340 Ciudad de México, Mexico

*e*Área de Química Aplicada, Departamento de Ciencias Básicas, Universidad Autónoma Metropolitana-Azcapotzalco, 02200 Ciudad de México, Mexico

*f*On Sabbatical as "Catedra Dr. Douglas Hugh Everett" at Departamento de Química, Universidad Autónoma Metropolitana-Iztapalapa, Avenida San Rafael Atlixco 186, Leyes de Reforma 1ra Sección, Iztapalapa, Ciudad de México 09310, Mexico

†Electronic supplementary information (ESI) available: Instrumental techniques and characterization. See DOI: https://doi.org/10.1039/d4dt01607f

‡These authors contributed equally to this manuscript.

Furthermore, MOF materials exhibit high kinetic and adsorption capacities in the adsorption process, demonstrating their immense potential for water remediation.[13] Fe-based MOFs show outstanding performance for TC adsorption, with an adsorption capacity of 420.6 mg g^{-1} for MIL-101(Fe).[14] However, most MOF materials applied for this purpose are synthesised using high energy.[15] Alternatively, MOF materials can be synthesised at room temperature using one of the routes of green methodologies.[16] Following this approach, MIL-100(Fe) displays high performance for fluoride adsorption.[17] MOF-808 shows selective adsorption for organic dyes.[18] Another alternative to improve the adsorption performance of a MOF material is the synthesis of a bimetallic MOF. For this, bimetallic materials of the MOF-74 family were reported for water treatment. CuCo-MOF-74 was applied for methylene blue degradation, highlighting the role of open metal sites.[19] FeCo-MOF-74 was used for arsenic removal, showing that the metal–oxygen groups played the main role in the interaction mechanism.[20] In these cases, the high density of open metal sites plays a vital role in the adsorption process in MOF-74 materials.

Based on this, the research is focused on applying room-temperature synthesis to an MOF-74 material to avoid high energy demand. It used two metal sources to synthesise a bimetallic material with open metal sites. Thus, a bimetallic ZnCu-MOF-74 was applied in the TC adsorption process from a water solution. The material was characterised using powder X-ray diffraction (PXRD), Fourier-transform infrared spectroscopy (FTIR), thermogravimetric analysis (TGA), N_2 adsorption, scanning electron microscopy (SEM), and X-ray photoelectron spectroscopy (XPS). The parameter optimisation, kinetics, adsorption isotherms, and thermodynamics are discussed for TC adsorption. The adsorption interaction between TC and ZnCu-MOF-74 was proposed in detail using XPS measurements. This work could provide further insight into applying a green MOF adsorbent to water treatment and the relevance of using open metal sites for the adsorption of water pollutants.

Experimental

Chemicals

Hydrate copper acetate ($Cu(CO_2CH_3)_2 \cdot H_2O$, 98%), dihydrate zinc acetate ($Zn(CH_3COO)_2 \cdot 2H_2O$, ≥98%), 2,5-dihydroxyterephthalic acid (H$_4$DHTP, 95%), tetracycline ($C_{22}H_{24}N_2O_8 \cdot H_2O$, 98%), methanol ($CH_3OH$, 99.8%), N,N-dimethylformamide (DMF, ≥99.8%), nitric acid (HNO_3, 70%), and sodium hydroxide pellets (NaOH, 97%) were supplied by Sigma-Aldrich. High-purity deionised water with a specific resistance of 18.2 mΩ cm^{-1} was obtained from a Milli-Q system Simplicity®. All reagents and solvents were used as received from commercial suppliers without further purification.

Synthesis of ZnCu-MOF-74

The synthesis was conducted as previously reported.[21] First, solution A was prepared with 1 mmol (0.1981 g) of the organic

linker H$_4$DHTP (2,5-dihydroxyterephthalic acid) in 10 mL of DMF (N,N-dimethylformamide). In parallel, solution B was prepared using 1 mmol of hydrate copper acetate and 1 mmol of dihydrate zinc acetate, which was dissolved in 10 mL of DMF. Solution B was added to solution A dropwise and then the solution was stirred at room temperature for 20 h. Finally, the precipitate was recovered by centrifugation, washed two times with DMF and three times with methanol, and soaked in methanol for six days, changing the solvent to fresh methanol every 2 days.

Instruments

Detailed information on the instrumental techniques is available in section S1.†

Adsorption experiments

Experiments were performed in triplicate to evaluate the impact of various factors on TC adsorption. The adsorption study of TC was carried out at room temperature. The influence of pH, mass, time, and concentration was studied. Each experiment was performed with 30 mL of TC solution at a specific concentration. The conditions were adjusted accordingly to understand the effect of experimental parameters. After adsorption, the material was separated by centrifugation (8000 rpm for 8 min). The reusability was studied for four adsorption–desorption cycles. TC was quantified in a UPLC Acquity system, consisting of a quaternary pump coupled to an FTN auto-sampler, a 2998 PDA detector, and a 2475 fluorescence detector from Waters™. Chromatograms were recorded in both detectors (PDA and FLR). In PDA, λ_{max} was recorded at 268 nm with a resolution of 4.8 nm, while in FLR, λ_{ex} and λ_{em} were recorded at 375 and 475 nm, respectively. Samples were separated on an ACQUITY UPLC® BEH C18 1.7 μm (2.1 × 50 mm) column at 35 °C with an isocratic regime (0.3 mL min^{-1}). The mobile phase composition was (30%) CH_3OH/(70%) 10 mM [HO_2CCO_2H]. Under these conditions, the retention time for tetracycline was 1.15 min, with a total run time for each sample of 3 min.

Results and discussion

Characterisation of ZnCu-MOF-74

The phase purity of bimetallic ZnCu-MOF-74 was confirmed using PXRD. The pattern (Fig. 1a) shows the characteristic peaks of the reported data,[21] which agrees with the monometallic version of Zn-MOF-74.[22] The functional groups were studied using FTIR analysis (Fig. 1b). A broad peak at 3403 cm^{-1} is observed related to the H–O–H stretching vibration, which can belong to –OH of the organic linker and adsorbed water molecules in the pores of ZnCu-MOF-74. The peaks at 1557 and 1420 cm^{-1} are associated with the symmetric and asymmetric stretching vibrations of C=O, respectively. The band at 1251 cm^{-1} is ascribed to the stretching vibration of C–O. This band corroborates the coordination with the metal centres. Then, the band at 587 cm^{-1} is related
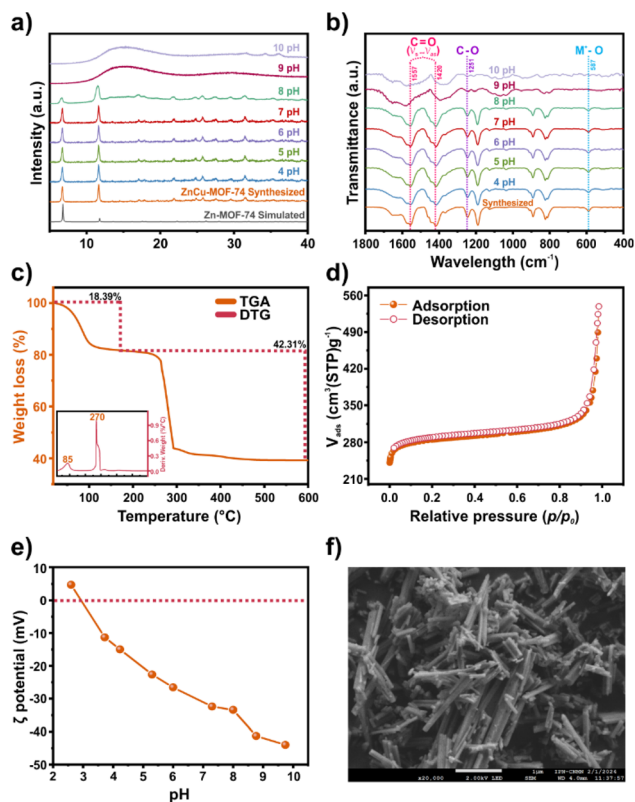
Fig. 1 (a) PXRD diffractogram; (b) FT-IR spectra; (c) TGA–DTG analysis; (d) N$_2$ isotherm adsorption; (e) zeta potential; and (f) SEM micrographs of ZnCu-MOF-74 synthesized.

Parameter optimisation: pH solution and mass adsorbent dosage

TC adsorption experiments were performed using the batch method. The effect of the pH solution on the adsorption process was analysed in the 4–10 pH range (Fig. 2a). Since water sources show a wide variety of pH values and the TC structure exhibits distinct speciation, pH is a crucial parameter to consider. Due to the acidic–basic nature of the solution, the TC structure displays three pK_a values at 3.3, 7.68, and 9.68 related to cationic, zwitterionic, and anionic species, respectively (Fig. S4†).[26]

The results indicate a similar adsorption capacity in the 4–8 pH range. However, an adsorption decrease is shown in the 9–10 pH range. Above the isoelectric point, pH 2.9, a negatively charged surface is observed. Considering the tetracycline speciation diagram (Fig. S3†), at pH 8, the TC structure is negatively charged. This would suppose repulsion between the ZnCu-MOF-74 surface and tetracycline molecules. However, considering the pH stability analysis from PXRD (Fig. 1a), it is assumed that the decrease in adsorption capacity is related to the collapse of the ZnCu-MOF-74 structure. Therefore, it is
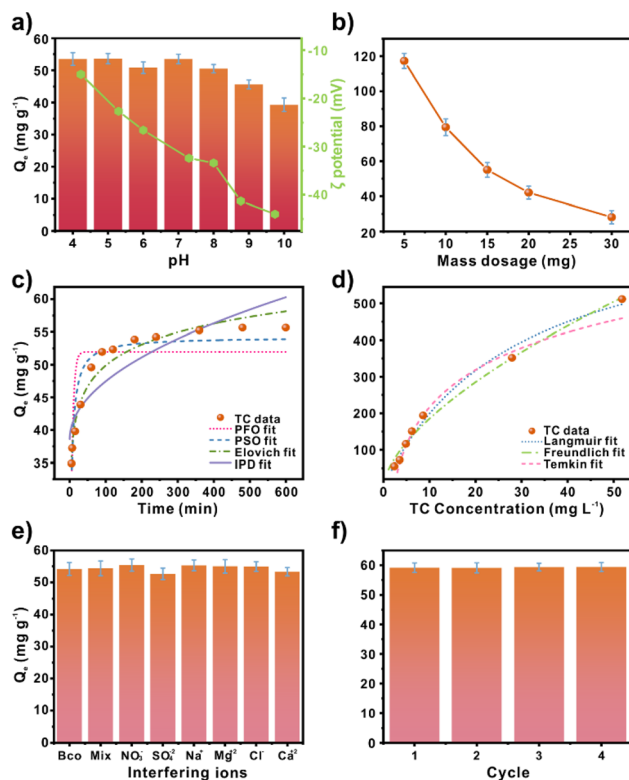
to the metal–oxygen bond.[23] The thermal stability was evaluated using thermogravimetric analysis (TGA) and derivative thermogravimetry (DTG) studies (Fig. 1c). The decomposition interval temperature was observed to be 245 to 320 °C, similar to the mono-metallic version of Zn and Cu-MOF-74,[24] indicating the distribution of heterogeneous metal centres in the sample.

Then, to determine the metal ratio in ZnCu-MOF-74, a chemical analysis by ICP-OES was conducted. A Zn/Cu ratio of 0.83 confirmed both metals' presence within the MOF. From the nitrogen isotherm (Fig. 1d) at 77 K, the BET surface area and pore volume were calculated to be 1142 m^2 g^{-1} and 0.81 cm^3 g^{-1}, respectively. Furthermore, based on the application of ZnCu-MOF-74 in water remediation, it was essential to determine the ζ potential (Fig. 1e). From this, an isoelectric point at pH 2.9 was found. A negative surface charge is observed beyond the isoelectric point. In addition, the stability of ZnCu-MOF-74 in water solution at different pH values (4–8) was confirmed using PXRD and FTIR (Fig. 1a and b). The surface morphology was analysed using a scanning electron microscope (SEM) (Fig. 1f), showing irregular chalk crystal pieces similar to those reported previously.[25] Besides, the elemental map (Fig. S1b†) indicates a homogeneous distribution of carbon, oxygen, copper, and zinc over the surface.

Fig. 2 (a) pH solution effect [15 mg, 30 ml, 30 mg L^{-1}, 4–10 pH, 10 h]; (b) adsorbent mass effect [5–30 mg, 30 ml, 30 mg L^{-1}, 6.5 pH, 10 h]; (c) kinetic fits [45 mg, 90 ml, 30 mg L^{-1}, 6.5 pH, 10 h]; (d) isotherm fits [15 mg, 30 ml, 30–300 mg L^{-1}, 6.5 pH, 10 h]; (e) TC adsorption in the presence of interfering ions compared to a control experiment (Bco) [15 mg, 30 ml, 30 mg L^{-1}, 6.5 pH, 10 h], and (f) TC adsorption–desorption in regenerated ZnCu-MOF-74 [15 mg, 30 ml, 30 mg L^{-1}, 6.5 pH, 10 h].

assumed that electrostatic interactions do not influence adsorption. The optimum pH range was determined from 4 to 8 pH. For this, the adsorption interactions could be related to π interactions. The π–π stacking from the π-electron density of the benzene rings and the TC structure is potentially the dominant interaction.[27]

Then, the effect of the MOF mass dosage (5–30 mg) on adsorption was evaluated (Fig. 2b). An adsorption reduction can be found with the mass increment, with a maximum and minimal adsorption capacity of 117 and 28 mg g^{-1}, respectively. 15 mg adsorbent mass was employed for the rest of the studies.

Adsorption kinetics and adsorption isotherms

Furthermore, the impact of contact time was tested (Fig. 2c). The kinetic results show, at first, accelerated adsorption at 60 min, achieving 49.58 mg g^{-1} of adsorption capacity. Afterward, it followed a slow stage until it reached equilibrium at 360 min. Non-linear fits were performed to determine the TC interactions. Four kinetic models, the pseudo-first-order model (PFO), the pseudo-second-order model (PSO), the Elovich model, and the intraparticle diffusion model (IPD) were evaluated. The parameters obtained are summarised in Table S4.† The PSO and Elovich models are the most suitable for adsorption, based on the correlation coefficients (R^2) of 0.904 and 0.957, respectively. The PSO and Elovich models suggest chemisorption.[28] Besides, the adsorption capacity estimated by PSO was very close to that obtained experimentally (54.22 and 55.64 mg g^{-1}, respectively). The Elovich model describes systems that have heterogeneous surfaces. This supports the possible π–π interactions suggested by the pH evaluation.[27]

Moreover, non-linear fits of the Langmuir, Freundlich, and Temkin models were carried out (Fig. 2d). The equations (Table S2†) and parameters (Table S5†) can be found in the ESI.† Based on the R^2, the best-fit order was Langmuir > Freundlich > Temkin, 0.990, 0.989, and 0.927, respectively. The maximum adsorption capacity estimated by Langmuir was 775.66 mg g^{-1} for ZnCu-MOF-74. This value is excellent compared to other MOF-based adsorbents for TC (Table S3†). The material outperformed MIL-101(Fe), a well-known mesoporous material (332 mg g^{-1}). However, the synthesis process for Fe-based MOF materials is low-cost.[29,30] The synthesis cost of ZnCu-MOF-74 is relatively high due to the cost of the organic linker. To avoid the energy cost of increased temperatures, room-temperature synthesis was selected. Furthermore, Cu metal is not classified as a potentially carcinogenic element.[31]

Effect of coexisting pollutants and reusability

TC adsorption with interfering ions such as NO_3^-, SO_4^{2-}, Na^+, Mg^{2+}, Cl^-, and Ca^{2+}, and a mixture that contained all of them were analysed (Fig. 2e). After examining the results and based on the control test (Bco), which only contains TC, a negligible variation was observed in the adsorption capacity. Furthermore, adsorption–desorption experiments were performed, employing methanol as a desorbing solvent (Fig. 2f).

The adsorption capacity performance remained constant in the four cycles evaluated. Furthermore, the chemical stability of the material was verified using PXRD, FTIR, and ICP-OES analysis. PXRD analysis after the adsorption process and the four cycle evaluation (Fig. S6†) confirmed that the material maintained its crystalline structure. FTIR shows the characteristic bands of ZnCu-MOF-74 (Fig. S7†), demonstrating that the functional groups are conserved. Also, the remaining solution after the adsorption process and the cyclability test was analysed to corroborate the stability fully. FTIR spectroscopy was conducted in the liquid phase (Fig. S8†). It was observed that only the bands of the TC molecule were detected. Then, the ICP-OES analysis of the solution revealed that 2.06 and 2.37 wt% Cu were found after the adsorption and cyclability tests, respectively. These results suggest that the material is stable in an aqueous solution for TC adsorption.

Thermodynamic analysis

The temperature influence (25–60 °C) was analysed. An increase in adsorption capacity can be noted jointly with the temperature increment (Fig. S5a†). Through the linear fit of Ln(K_c) against T^{-1} (Fig. S5b†), it was possible to determine enthalpy (ΔH), entropy (ΔS), and Gibbs free energy (ΔG). The positive values of ΔH and ΔS, 38.45 and 0.14 kJ mol^{-1}, respectively, describe an endothermic adsorption process and increased randomness in the adsorption.[32] Conversely, the negative ΔG value obtained denotes spontaneous adsorption.[33]

Adsorption mechanism

FTIR and XPS were employed further to analyse the adsorption mechanism (Fig. 3). The FTIR spectra before and after the TC adsorption (Fig. 3a) are very similar. Only a decrease in intensity is observed, which could be related to π–π stacking due to the presence of benzene rings.[27] Then, the survey analysis (Fig. 3b) confirms the presence of N 1s due to the adsorption of TC. The high-resolution XPS spectra of Zn 2p (Fig. 3c) show a relevant shift (0.5 eV) in the Zn 2p$_{3/2}$ binding energy from 1022.2 to 1021.7 eV after the adsorption. Similarly, the high-resolution XPS spectra of Cu 2p (Fig. 3d) display a peak at 935.0 eV related to Cu^{2+}. The peak shifts (0.6 eV) to 934.4 eV after the TC adsorption. These shifts in the binding energies for Cu and Zn 2p to lower values can be related to a change in the chemical environment of the metal centres in ZnCu-MOF-74. A complex between the oxygen/nitrogen functional groups of the TC structure and metal centres could be formed *via* coordinated bonds.[14] The high-resolution XPS spectra of C 1s (Fig. 3e) exhibit peaks at 284.4, 285.8, 288.4, and 290.1 eV related to C=C in the aromatic rings, C–OH, –C=O and π–π*. After TC adsorption, the peaks shift to 284.3, 285.9, 288.0, and 290.0 eV, respectively. An evident change (0.4 eV) in the binding energy at lower energy was observed for the peak associated with –C=O. It can be related to the π–π stacking since TC interacts with the carbonyl group from the organic linker of ZnCu-MOF-74.[19] The changes in the O 1s spectra supported this. The high-resolution XPS spectra of O 1s (Fig. 3f)
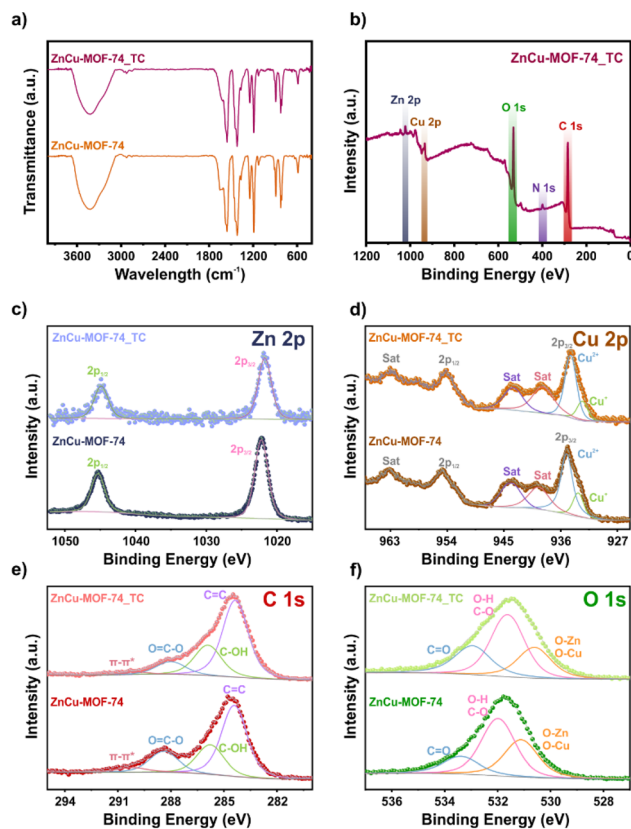
Fig. 3 (a) FTIR before and after TC adsorption; (b) XPS survey spectrum of exhausted ZnCu-MOF-74; high-resolution spectra before and after TC adsorption of (c) Zn 2p, (d) Cu 2p, (e) C 1s, and (f) O 1s.

display peaks at 531.1, 532.0, and 533.4 eV related to M–O/C=O, C–OH, and H$_2$O, respectively. After TC adsorption, the peaks shifted to 530.6, 531.6, and 533.0 eV. The changes in the peaks of M–O/C=O (0.5 eV) and C–OH (0.4 eV) at lower energies are associated with the increase in electron density due to the presence of the TC molecule.[34]

Conclusions

A bimetallic MOF ZnCu-MOF-74 was synthesised at room temperature, avoiding high energy demand. The material was thoroughly characterised using diverse spectroscopic techniques. ZnCu-MOF-74 exhibits outstanding TC adsorption performance with a Langmuir maximum adsorption capacity of 775.6 mg g^{-1}. The material shows high stability and adsorption capacity in the pH 4–8 range. Kinetic and adsorption data fitted to the Elovich and Langmuir models suggest a physicochemical adsorption process. The thermodynamic analysis confirms the endothermic nature of the adsorption. Excellent cyclability was observed for four adsorption–desorption cycles with high stability. The main adsorption mechanism was proposed using FTIR and XPS measurements. The primary interactions are the π–π stacking and chemical complexation between the TC molecule and ZnCu-MOF-74. Overall, this

study demonstrates the synthesis of a novel room-temperature bimetallic MOF, ZnCu-MOF-74, for efficient and effective TC removal from water, and further studies need to be carried out with direct wastewater studies for real-world applications.

Data availability

The data supporting this article have been included as part of the ESI.†

Conflicts of interest

There are no conflicts to declare.

Acknowledgements

References

1 R. I. L. Eggen, J. Hollender, A. Joss, M. Schärer and C. Stamm, *Environ. Sci. Technol.*, 2014, **48**, 7683–7689.
2 M. Schaffner, H.-P. Bader and R. Scheidegger, *Sci. Total Environ.*, 2009, **407**, 4902–4915.
3 O. M. Rodriguez-Narvaez, J. M. Peralta-Hernandez, A. Goonetilleke and E. R. Bandala, *Chem. Eng. J.*, 2017, **323**, 361–380.
4 M. Taheran, M. Naghdi, S. K. Brar, M. Verma and R. Y. Surampalli, *Environ. Nanotechnol., Monit. Manage.*, 2018, **10**, 122–126.
5 I. Alderton, B. R. Palmer, J. A. Heinemann, I. Pattis, L. Weaver, M. J. Gutiérrez-Ginés, J. Horswell and L. A. Tremblay, *Emerging Contam.*, 2021, **7**, 160–171.
6 M. E. Lindsey, M. Meyer and E. M. Thurman, *Anal. Chem.*, 2001, **73**, 4640–4646.
7 R. Acosta, V. Fierro, A. Martinez De Yuso, D. Nabarlatz and A. Celzard, *Chemosphere*, 2016, **149**, 168–176.
8 R. Zandipak and S. Sobhanardakani, *Clean Technol. Environ. Policy*, 2018, **20**, 871–885.
9 H.-C. "Joe" Zhou and S. Kitagawa, *Chem. Soc. Rev.*, 2014, **43**, 5415–5418.
10 J. L. Obeso, J. G. Flores, C. V. Flores, V. B. López-Cervantes, V. Martínez-Jiménez, J. A. De Los Reyes, E. Lima, D. Solis-Ibarra, I. A. Ibarra, C. Leyva and R. A. Peralta, *Dalton Trans.*, 2023, **52**, 12490–12495.
11 J.-R. Li, R. J. Kuppler and H.-C. Zhou, *Chem. Soc. Rev.*, 2009, **38**, 1477.

12 M. J. Kalmutzki, C. S. Diercks and O. M. Yaghi, *Adv. Mater.*, 2018, **30**, 1704304.

13 X. Tang, C. Zhou, W. Xia, Y. Liang, Y. Zeng, X. Zhao, W. Xiong, M. Cheng and Z. Wang, *Chem. Eng. J.*, 2022, **446**, 137299.

14 Z. Zhang, Y. Chen, Z. Wang, C. Hu, D. Ma, W. Chen and T. Ao, *Appl. Surf. Sci.*, 2021, **542**, 148662.

15 M. H. Yap, K. L. Fow and G. Z. Chen, *Green Energy Environ.*, 2017, **2**, 218–245.

16 S. Dai, A. Tissot and C. Serre, *Bull. Chem. Soc. Jpn.*, 2021, **94**, 2623–2636.

17 W. Li, T. Zhang, L. Lv, Y. Chen, W. Tang and S. Tang, *Colloids Surf., A*, 2021, **624**, 126791.

18 H. Su, J. Hou, J. Zhu, Y. Zhang and B. Van Der Bruggen, *Sep. Purif. Technol.*, 2024, **333**, 125957.

19 H. Li, Z. Yang, S. Lu, L. Su, C. Wang, J. Huang, J. Zhou, J. Tang and M. Huang, *Chemosphere*, 2021, **273**, 129643.

20 J. Sun, X. Zhang, A. Zhang and C. Liao, *J. Environ. Sci.*, 2019, **80**, 197–207.

21 J. G. Flores, J. Aguilar-Pliego, N. Martin-Guaregua, I. A. Ibarra and M. Sanchez-Sanchez, *Catal. Today*, 2022, **394–396**, 295–303.

22 J. L. C. Rowsell and O. M. Yaghi, *J. Am. Chem. Soc.*, 2006, **128**, 1304–1315.

23 Z. Gao, L. Liang, X. Zhang, P. Xu and J. Sun, *ACS Appl. Mater. Interfaces*, 2021, **13**, 61334–61345.

24 J. G. Flores, M. Díaz-García, I. A. Ibarra, J. Aguilar-Pliego and M. Sánchez-Sánchez, *J. Solid State Chem.*, 2021, **298**, 122151.

25 H. Abedini, A. Shariati and M. R. Khosravi-Nikou, *Chem. Eng. Res. Des.*, 2020, **153**, 96–106.

26 C. Gu and K. G. Karthikeyan, *Environ. Sci. Technol.*, 2005, **39**, 2660–2667.

27 J. Xia, Y. Gao and G. Yu, *J. Colloid Interface Sci.*, 2021, **590**, 495–505.

28 É. C. Lima, M. A. Adebayo and F. M. Machado, in *Carbon Nanomaterials as Adsorbents for Environmental and Biological Applications*, ed. C. P. Bergmann and F. M. Machado, Springer International Publishing, Cham, 2015, pp. 33–69.

29 Y. Dong, T. Hu, M. Pudukudy, H. Su, L. Jiang, S. Shan and Q. Jia, *Mater. Chem. Phys.*, 2020, **251**, 123060.

30 M. Beiranvand, S. Farhadi and A. Mohammadi-Gholami, *RSC Adv.*, 2022, **12**, 34438–34453.

31 H. Zheng, Y. Zhou, D. Wang, M. Zhu, X. Sun, S. Jiang, Y. Fan, D. Zhang and L. Zhang, *Colloids Surf., A*, 2022, **651**, 129640.

32 A. T. Ojedokun and O. S. Bello, *Appl. Water Sci.*, 2017, **7**, 1965–1977.

33 S. M. Mirsoleimani-azizi, P. Setoodeh, S. Zeinali and M. R. Rahimpour, *J. Environ. Chem. Eng.*, 2018, **6**, 6118–6130.

34 Z. Guo, J. Zhou, H. Hou, X. Wu and Y. Li, *J. Solid State Chem.*, 2023, **323**, 124059.